

SFTS Virus Infection in Nonhuman Primates

Cong Jin,^{1,a} Hong Jiang,^{2,a} Mifang Liang,¹ Ying Han,^{1,3,b} Wen Gu,^{1,b} Fushun Zhang,¹ Hua Zhu,² Wei Wu,¹ Ting Chen,² Chuan Li,¹ Weilun Zhang,² Quanfu Zhang,¹ Jing Qu,¹ Qiang Wei,² Chuan Qin,² and Dexin Li¹

¹Key Laboratory for Medical Virology, NHFPC, National Institute for Viral Disease Control and Prevention, China CDC, and ²Laboratory of Virus, Institute of Laboratory Animal Science, Chinese Academy of Medical Sciences, Beijing, and ³Wenzhou Medical University, China

SFTS virus (SFTSV) is a highly pathogenic bunyavirus that causes severe fever with thrombocytopenia syndrome (SFTS), an emerging infectious disease in China. Laboratory mice have been reported to be susceptible to SFTSV infection, but the infection in nonhuman primates has not been investigated. This study is the first to report that, in rhesus macaques, SFTSV does not cause severe symptoms or death but causes fever, thrombocytopenia, leukocytopenia, and increased levels of transaminases and myocardial enzymes in blood. Viremia, virus-specific immunoglobulin M and immunoglobulin G antibodies, and neutralizing antibodies were identified in all infected macaques. Levels of the cytokines interferon γ , eotaxin, tumor necrosis factor α , and macrophage inflammatory protein 1 β were significantly elevated in the blood. Minor pathological lesions were observed in the liver and kidney during the late stages of infection. Overall, SFTSV infection in rhesus macaques resembled mild SFTS in humans.

Keywords. SFTS virus; infectious animal model; nonhuman primate; pathogenesis.

Severe fever with thrombocytopenia syndrome (SFTS) is an emerging infectious disease caused by SFTS virus, a novel phlebovirus in the family of Bunyaviridae [1, 2]. SFTS is believed to be transmitted to humans through tick bites [1, 3], and several cases of person-to-person transmission have been reported [4, 5]. Clinical features of SFTS typically include abrupt fever; thrombocytopenia; leukocytopenia; gastrointestinal symptoms; elevated serum levels of alanine aminotransferase (ALT), aspartate aminotransferase (AST), blood urea nitrogen, creatinine, lactate dehydrogenase, and creatine kinase; and elongated activated partial-thromboplastin time [4, 6], indicating impairment in multiple organs. SFTSV infection can also induce a cytokine storm with abnormally expressed

cytokine profiles in the acute phase of viral infection [7]. Patients with severe SFTS usually die from multiple organ dysfunction syndromes and disseminated intravascular coagulation within 2 weeks after onset of the disease [4, 6]. The average case-fatality rate is about 10% for hospitalized individuals [8, 9].

After the discovery of SFTS in China, several cases with similar clinical symptoms were identified in the United States, Japan, India, and Korea [10–13]. Phylogenetic analysis showed that Korean isolates and Japanese isolates from SFTS cases were closely related to the SFTSV strains identified in China. The Heartland virus isolated in the United States and the Malsoor virus isolated in India shared the highest homology with SFTSV. Although epidemics of SFTSV infection have been revealed outside of China, there are no licensed vaccines or specific pharmaceutical options approved for human use.

Developing adequate animal models for SFTSV is a research priority for understanding the pathogenesis of this emerging viral pathogen and for developing countermeasures to infection. It has been reported that laboratory rodents, such as mice and hamsters, are susceptible to SFTSV infection through various inoculation routes, including intramuscular, subcutaneous, intravascular, or intraperitoneal injection, leading to viremia and strong antibody responses [14]. Moreover,

Received 12 February 2014; accepted 12 August 2014; electronically published 17 October 2014.

^aC. J. and H. J. contributed equally to this work.

^bPresent affiliations: Children's Hospital, Zhejiang University, Hangzhou (Y. H.), and National Institute of Environmental Health and Related Product Safety, Chinese Center for Disease Control and Prevention, Beijing (W. G.), China.

Correspondence: Dexin Li, PhD, National Institute for Viral Disease Control and Prevention, China CDC, 155 Changbai Road, Changping District, Beijing 102206, China (lidx@chinacdc.cn).

The Journal of Infectious Diseases® 2015;211:915–25

© The Author 2014. Published by Oxford University Press on behalf of the Infectious Diseases Society of America. All rights reserved. For Permissions, please e-mail: journals.permissions@oup.com.

DOI: 10.1093/infdis/jiu564

SFTSV infection in C57/BL6 mice caused symptoms of thrombocytopenia, leukocytopenia, and elevated levels of AST, ALT, and blood urea nitrogen in blood, as well as pathological lesions in the spleen, liver, and kidney. The susceptibility to SFTSV infection may vary depending on the strain of rodents used [14]. SFTSV infection did not cause the death of immune competent mice and hamsters and, overall, resembled a mild infection in humans.

Nonhuman primates are the gold standard animal models for studying the pathogenesis of viral human diseases and for developing countermeasures [15–17]. Nonhuman primates have been widely used to study the infection and pathogenesis of bunyaviruses that lead to disease involving hemorrhagic fever [18–21]. However, to date, there have been no studies performed on SFTSV infection in nonhuman primates. In this study, we use Asian rhesus macaques (*Macaca mulatta*) to examine SFTSV infection in nonhuman primates. We report the characteristics of infection kinetics and viremia, virus-specific antibody responses, and inflammatory cytokine responses over the entire experimental infection course, as well as pathological lesions observed at the study end point, in SFTSV-infected rhesus macaques.

MATERIALS AND METHODS

Virus and Animals

The SFTSV strain HB29 was isolated from an individual with a severe case of SFTS by plaque purification and was propagated 5 passages in Vero E6 cells. Eight healthy adult female rhesus macaques (age range, 4–5 years; weight range, 4.1–5.2 kg) were purchased from Sichuan Yibin Hengshu Biotechnology. All macaques were proven to be absent of previous infections of *Mycobacterium tuberculosis*, *Salmonella* species, *Shigella* species, ectoparasites, endoparasites, and SFTSV. Of the 8 macaques, 6 (MK1–6) were subjected to SFTSV infection, and 2 (MK-C1 and MK-C2) were control animals. Among the 6 infected macaques, 2 (MK5 and MK6) were euthanized after 2 weeks of infection, and 4 (MK1–4) were euthanized after 4 weeks of infection.

Animal Infection and Blood Sample Collection

Animals were anesthetized by means of ketamine hydrochloride (5 mg/kg) and then received an intramuscular injection of 1×10^7 median tissue culture infective doses (TCID₅₀) of SFTSV in 1 mL of saline. The same volume of saline was injected into control animals. Infected macaques were monitored daily for abnormal appearance and behaviors. On days 0, 1, 3, 5, 7, 9, 12, 15, 19, 23, and 28 after inoculation, the animals were measured for weight and rectal temperature. For blood sampling, 6–8 mL of venous blood was collected on days 0, 1, 3, 5, 7, and 9, and 8–10 mL of venous blood was collected on days 12, 15, 19, 23, and 28.

Hematological and Biochemical Parameters

Counts of white blood cells (WBCs), red blood cells, and platelets and levels of hemoglobin were measured in blood samples stored in ethylenediaminetetraacetic acid, using a Mindray 3000 hematology analyzer (Mindray Limited). The plasma levels of sodium, potassium, AST, ALT, blood urea nitrogen, creatinine, creatine kinase, lactate dehydrogenase, alkaline phosphatase, and cystatin C were measured using a Hitachi 7080 biochemical analyzer (Hitachi Limited).

Virus Detection in Blood and Tissues

Viral RNA copies were measured using a TaqMan 1-step real-time reverse transcription polymerase chain reaction (PCR) assay as previously described [22]. Infectious viral titers in blood and tissues were determined by a TCID₅₀ assay as previously reported [1, 14].

Antibody and Cytokine Assays

SFTSV-specific immunoglobulin M (IgM) and immunoglobulin G (IgG) antibodies were quantified by a Luminex assay as previously described [14], using R-phycoerythrin-conjugated goat anti-monkey IgG (Sigma Aldrich) or R-phycoerythrin-conjugated rat anti-monkey IgM monoclonal antibody (Abcam) as secondary antibodies. The neutralizing antibody titer was measured by means of a microneutralization assay as previously described [1, 4]. A commercial multiplex-biometric immunoassay kit was used to test production of 22 nonhuman primate cytokines in plasma (Affymetrix), including interleukin 1 β , interleukin 2, interleukin 4, interleukin 5, interleukin 6, interleukin 9, interleukin 10, interleukin 12, interleukin 13, interleukin 15, eotaxin, granulocyte colony-stimulating factor, granulocyte macrophage colony-stimulating factor, interferon γ (IFN- γ), IFN- γ -inducible protein, monocyte chemotactic protein 1, macrophage inflammatory protein 1 α , macrophage inflammatory protein 1 β , platelet-derived growth factor, regulated on activation and normally T-cell expressed, tumor necrosis factor α , and vascular endothelial growth factor.

Tissue Sample Collection and Histopathological Analysis

At the study end point, animals were subjected to necropsy after exsanguination. Spleen, lymph node, liver, kidney, intestine, lung, muscle, brain, and heart tissue specimens were collected. For each type of tissue, half of the specimen was immersion fixed in 10% neutral buffered formalin for histopathological examination, and half was frozen at -80°C for virological assays. Paraffin-embedded tissue sections were subjected to hematoxylin-eosin staining for blinded histopathology examination by two pathologists. Histopathological evaluation of the liver was performed using the HAI-Knodell scoring system [23]. Glomerular lesions in the kidney were evaluated using a scoring system developed previously [24], which evaluated glomerular lesions for the presence or absence of tuft atrophy, Bowman capsule

changes, periglomerular fibrosis, membranoproliferative changes, tuft adhesions, sclerosis, and/or atrophy. Lesion scores were assigned as follows: 0, no lesions; 1, <10% of the total slide area affected; 2, 10%–25%; 3, 25%–50%; and 4, >50% [24].

Animal Ethics

All SFTSV infectious animal experiments were performed in biosafety level 3 containment at the Institute of Laboratory Animal Science of the Chinese Academy of Medical Sciences in accordance with institutional guidelines. The animal study protocol was approved by the institutional animal welfare committee.

RESULTS

SFTSV Induced Fever and Changes of Hematological and Biochemical Parameters

To investigate the kinetics of SFTSV infection in 6 rhesus macaques, weight, temperature, and hematological and biochemical parameters were tested before virus inoculation (day 0) and on days 1, 3, 5, 7, 9, 12, 15, 19, 23, and 28 after inoculation. Daily observation found no abnormal appearance or behavior. During the early stage of infection, from days 1 to 7 after inoculation, all 6 infected macaques developed mild temperature increase and decreased counts of white blood cells and platelets, which mimicked the typical clinical symptoms of fever, thrombocytopenia, and leukocytopenia in patients with SFTS (Figure 1). Additionally, decreased red blood cell counts and decreased hemoglobin concentrations were observed, both of which have been reported in some patients with SFTS as minor symptoms [25]. Blood biochemistry analysis showed substantially elevated levels of myocardial enzyme lactate dehydrogenase and AST from days 5 to 12 after inoculation in infected macaques, as reported in most patients with SFTS [4, 6] (Figure 1). Elevated levels of ALT were observed in 2 infected macaques (MK1 and MK5) from days 5 to 12 after inoculation, and a mild increase in the creatinine level was seen in 4 infected macaques (MK1–3 and MK6) from days 1 to 5 after inoculation. Mild increases in levels of both ALT and creatinine have been reported in some patients [4, 6]. Overall, the exposure of rhesus macaques to SFTSV mimicked the major clinical features of a mild infection in patients with SFTS (Table 1).

Viremia and Virus-Specific Antibody Responses

To verify SFTSV infection in macaques, viral RNA copies, viral titers, and virus-specific antibody responses were analyzed at various time points. We found that the number of viral RNA copies in blood began to increase on day 1, peaked during days 3–5, and were undetectable on day 7 after inoculation (Figure 2). Viral titers during peak viremia ranged from $10^{1.6}$ to $10^{4.1}$ TCID₅₀/mL (Supplementary Table 1). In SFTSV-infected macaques, virus-specific IgM antibodies appeared on day 5 after inoculation, remained at high levels from days 7 to 15 after

inoculation, and then gradually decreased in abundance (Figure 2). Virus-specific IgG antibodies appeared later on day 7 after inoculation, and levels then gradually increased and plateaued around day 15 after inoculation (Figure 2). SFTSV infection in macaques also induced neutralizing antibody responses at low levels, ranging from 1:32 to 1:128 (Supplementary Table 1). Together, these data indicate that SFTSV can efficiently infect and replicate in macaques and is capable of inducing virus-specific antibody responses.

Abnormal Cytokine Profiles in Infected Rhesus Macaques

In the acute phase of SFTSV infection, disease severity is associated with an abnormal cytokine storm. Therefore, to study systemic host immune responses to SFTSV infection, we examined cytokine production in SFTSV-infected macaques throughout the experimental infection course (Figure 3). We found that, in infected macaques, the production of IFN- γ and eotaxin were significantly elevated during the early stage of infection and that the production of tumor necrosis factor α and macrophage inflammatory protein 1 β were significantly elevated during the late stage of infection. Additionally, 2 infected macaques (MK3 and MK6) showed increased production of interleukin 5 and granulocyte macrophage colony-stimulating factor between days 9 and 15 after inoculation. Two infected macaques (MK1 and MK4) showed increased production of interleukin 9 between days 19 and 28 after inoculation, one of which (MK4) showed increased production of the cytokines interleukin 10 and IFN- γ -inducible protein between days 19 and 28 after inoculation. The elevated production of inflammatory cytokines during the experimental infection course indicated that SFTSV infection induced systemic host antiviral immune responses in macaques.

Virus Distribution and Pathological Lesions in Tissues

To assess the tissue tropism of SFTSV, viral RNA copies were measured by a real-time PCR assay in spleen, lymph node, liver, kidney, intestine, lung, muscle, brain, and heart tissue specimens obtained at the end point of experimental infection. We found high viral RNA levels in the spleens of all 6 infected macaques and in the lymph nodes of all but 1 (MK2) infected macaques. Low levels of viral RNA were detected in the liver of 1 infected macaque (MK3), in the kidney of 3 infected macaques (MK3, MK4, and MK6), and in the intestine of 4 infected macaques (MK1, MK3, MK5, and MK6; Figure 4). Viral RNA was not detected in the lung, muscle, brain, or heart. A viral titer of $10^{4.1}$ TCID₅₀/mL was measured in the lymph nodes collected 2 weeks after virus inoculation from 1 macaque (MK5), suggesting that the lymph node might be the major organ for active replication of SFTSV in macaques and that lymph nodes collected at earlier time points could also be contagious. Viral antigens were not detected in viral RNA-positive tissue specimens by immunohistochemistry assays, which could be due to viral

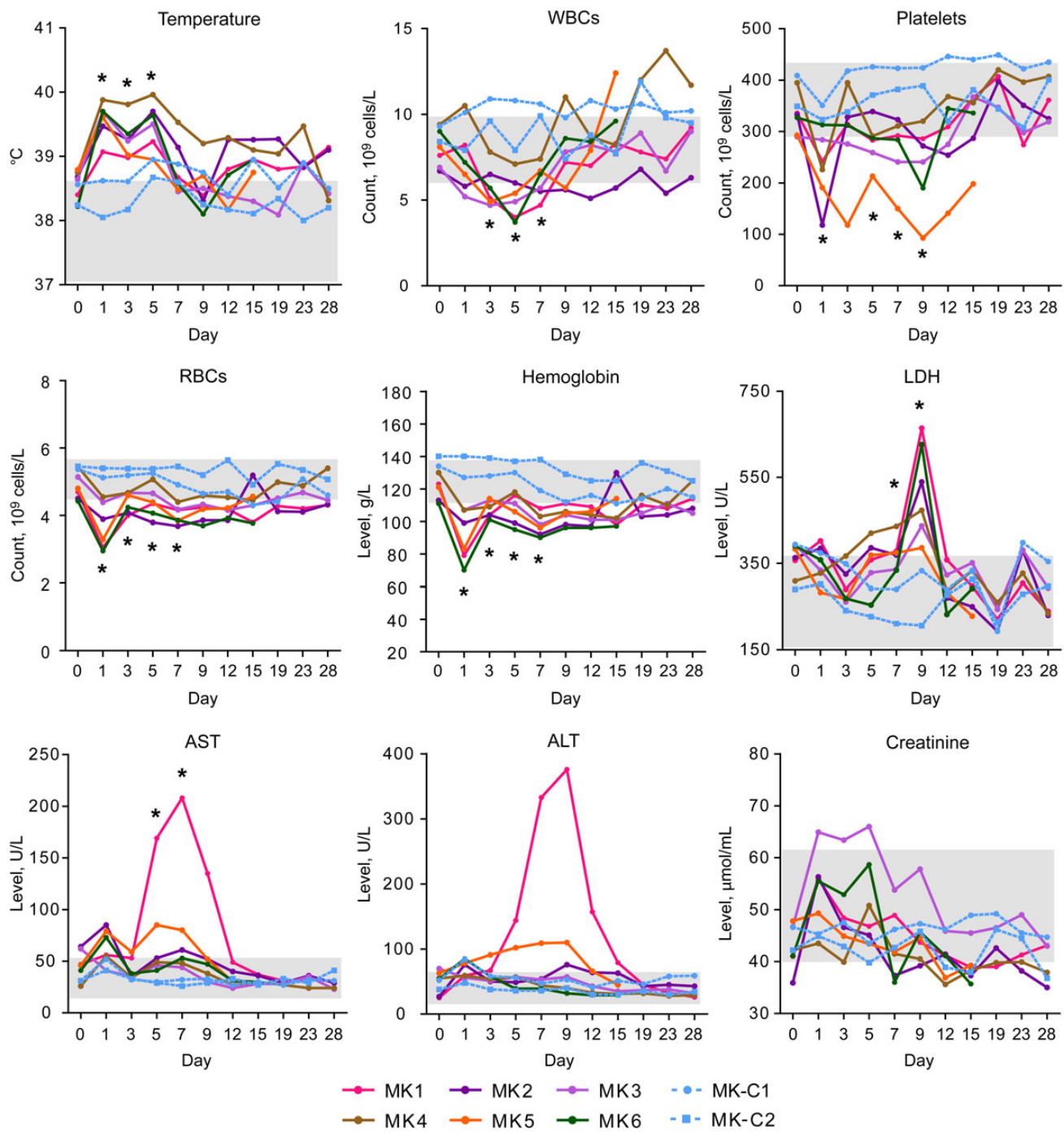


Figure 1. Kinetics of hematological and biochemical parameters in rhesus macaques following inoculation with SFTSV. Six rhesus macaques (MK1–6) were infected via intramuscular injection with 10^7 median tissue culture infective doses (TCID₅₀) of SFTSV. Two rhesus macaques (MK-C1 and MK-C2) were injected with saline as controls. Sample collection and analysis were performed at the indicated time points until animals were euthanized. In each graph, gray shadows indicate the physiological reference range of the parameter [26, 34–36]. * $P < .05$, between the infected group and the control group at a given time point. Abbreviations: ALT, alanine aminotransferase; AST, aspartate aminotransferase; LDH, lactate dehydrogenase; RBC, red blood cell; WBC, white blood cell.

clearance at the end point or the less sensitive detection limit of immunohistochemistry assays.

Gross pathological and histopathological lesions were also examined in the tissues collected from infected macaques. All

examined organs appeared normal by gross inspection. Major histopathological lesions were found in the liver and kidney (Figure 5). In SFTSV-infected livers (Figure 5C and 5E), multiple scattered loci of mild-to-moderate piecemeal necrosis and

Table 1. Comparison of SFTS Virus Infection Features and Kinetics in Nonhuman Primates, Mice, and Humans

	Nonhuman Primates	Mice [14]	Humans
General infection status			
Severity	Mild	Mild	Various from asymptomatic to death; case-fatality rate is around 10% [8, 9]
Major symptom(s)	Moderate fever lasts around 4 d	No abnormal appearance	High fever (>38°C) lasts around 3–7 d; gastrointestinal, hemorrhagic, CNS manifestations [1, 6]
Age, sex	4–5 y, female	3–4 wks, female	Median 58 y [8], 53.35% female [8]
Infection route	Intramuscular injection	Intramuscular injection	Tick bite, direct contact with infectious blood or body secretions [1, 4]
Viral exposure	1×10^7 TCID ₅₀ per animal	1×10^5 TCID ₅₀ per animal	NA
Peak viremia	$10^{4.3-5.8}$ RNA copies/mL during days 3–5	$10^{4.7-5.0}$ RNA copies/mL on day 1	Nonfatal: $10^{4.3-6.1}$ RNA copies/mL during days 3–7; fatal: $10^{6.6-8.0}$ copies/mL until death [7]
Host response^a			
WBC count	Decrease to 0.5-fold during days 3–7	Decrease to 0.6-fold during days 1–3	Decrease to 0.24- and 0.23-fold in nonfatal and fatal cases, respectively [7], during days 3–9 [6]
Platelet count	Decrease to 0.5-fold during days 1–9	Decrease to 0.5-fold during days 1–3	Decrease to 0.23- and 0.14-fold in nonfatal and fatal cases, respectively [7], during days 5–13 [6]
RBC count/Hb level	Decrease to 0.7-fold during days 1–7	NA	32.2% of patients showed decreased Hb concentration [25]
ALT level	Increase to 3.6-fold during days 5–12	Increase to 5.6-fold during days 7–14	Nonfatal: increase to 5-fold during days 7–13; fatal: increase to 13.7-fold and remain high until death [6, 7]
AST level	Increase to 3.5-fold during days 5–12	Increase to 3.3-fold during days 1–14	Nonfatal: increase to 5-fold during days 7–13; fatal: increase to 43.6-fold, with increase continuing until death [6, 7]
LDH level	Increase to 1.8-fold during days 5–12	NA	Nonfatal: increase to 2.3-fold, during days 7–13; Fatal: increase to 9-fold, with increase continuing until death [6, 7]
Creatinine level	Increase to 1.5-fold during days 1–5	NA	Increase to 1.4-fold in patients [7]
IgM expression	Positive: day 5; peak: day 7	Positive: day 3; peak: day 7	Positive around day 8 (range, days 4–14) [25]
IgG expression	Positive: day 7; peak: 2–3 wks	Positive: day 7; peak: 2–3 wks	Positive around day 12 (range, days 8–14) [25]
NAb titer	Low (1:32–1:128)	Low (1:10–1:80)	Moderate (1:80–1:640) [1]
Cytokines detected	IFN- γ , TNF- α , eotaxin, MIP-1 β , IL-10, IP-10, IL-5, GM-CSF, IL-9	NA	IFN- γ , TNF- α , MIP-1 β , IL-10, IP-10, IL-1RA, IL-6, G-CSF, MCP-1, PDGF-BB, RANTES, IL-1 β , IL-8, MIP-1 α [7]
Histopathological findings in lesions, by site^b			
Lymph node	Not obvious at late stages	NA	Lymphadenopathy (33%) [1]; necrotizing lymphadenitis, lymphocyte depletion, infiltration of histiocytes and immunoblasts, hemophagocytosis [13]
Spleen	Not obvious at late stages	Lymphocyte depletion, increase of phagocytes with platelets on day 3	Hemophagocytosis [13]
Liver	Multiple scattered loci of hepatocyte necrosis on days 14 and 28	Mild degeneration of hepatocytes and scattered necrosis on day 14	Increased liver enzyme levels (94%) [1]; mild inflammation with lymphocytes and macrophages around portal tracts [13]
Kidney	Glomerular hypercellularity, mesangial thickening, congestion in Bowman's space on days 14 and 28	Glomerular hypercellularity, mesangial thickening, congestion in Bowman's space on day 14	Hematuria (59%), proteinuria (84%), renal function impairment (13%) [1]; renal swelling, subepithelial hemorrhage [13]
Gastrointestinal tract	Not obvious at late stages	Not obvious	Fecal occult blood (21%) [1], tarry stool [13]
Bone marrow	Not obvious at late stages	Increase of megakaryocytes on day 3	Mildly hypocellular, increase of activated histiocytes and hemophagocytes [13]

Table 1 continued.

	Nonhuman Primates	Mice [14]	Humans
Virus detection in tissue ^b	Viral RNA: lymph node, spleen, liver, kidney, intestine	Viral RNA: spleen, liver, kidney; viral antigen: spleen	Viral RNA: lymph node, bone marrow, adrenal glands, liver, spleen [13]; viral antigen: lymph node, bone marrow, adrenal glands, liver, spleen [13]

Abbreviations: ALT, alanine aminotransferase; AST, aspartate aminotransferase; G-CSF, granulocyte colony-stimulating factor; GM-CSF, granulocyte macrophage colony-stimulating factor; Hb, hemoglobin; IFN- γ , interferon γ ; IgG, immunoglobulin G; IgM, immunoglobulin M; IL-1RA, interleukin 1RA; IL-1 β , interleukin 1 β ; IL-5, interleukin 5; IL-6, interleukin 6; IL-8, interleukin 8; IL-9, interleukin 9; IL-10, interleukin 10; IP-10, interferon γ -inducible protein; LDH, lactate dehydrogenase; MCP-1, monocyte chemoattractant protein 1; MIP-1 α , macrophage inflammatory protein 1 α ; MIP-1 β , macrophage inflammatory protein 1 β ; NA, not applicable; NAb, neutralizing antibody; PDGF-BB, platelet-derived growth factor; RANTES, regulated on activation and normally T-cell expressed; RBC, red blood cell; TCID₅₀, median tissue culture infective dose; TNF- α , tumor necrosis factor α ; WBC, white blood cell.

^a In nonhuman primates, the fold-change of parameter is calculated by first averaging the most altered values beyond the reference range in infected macaques to get the mean peak value, and then dividing the mean peak value by the mean value in mock macaques. In mice and humans, the fold-change of parameter is calculated by dividing the reported mean value in infected groups by the reported mean value in uninfected groups.

^b Based on findings from a fatal case [13].

bridging necrosis of hepatocytes were observed as multifocal pyknosis, karyorrhexis, and karyolysis. Mild hepatocyte degeneration and inflammatory cell infiltration was also seen in the liver. Major histopathological changes in SFTSV-infected kidneys included glomerular hypercellularity, mesangial thickening, and congestion in the Bowman space, with an absence of inflammatory cell infiltration (Figure 5D and 5F).

The histopathological lesions observed in SFTSV-infected rhesus macaques were similar to those observed in SFTSV-infected mice [14] (Table 1). However, in the infected macaques, histopathological scores, which reflect the severity of tissue lesions, were low (Supplementary Table 1). The low severity of pathological lesions in SFTSV-infected macaques could be due to the transient nature of pathological lesions that appear in the early phase of infection but resolve in the late phase of infection. Alternatively, the low-to-medium levels of viremia

and less severe infection features seen in infected macaques might preclude the development of severe pathological lesions in tissues.

End point analyses of virus distribution and histopathological lesions in infected macaques thus suggest that the spleen, lymph node, liver, kidney, and intestine may be involved in mediating virus-induced pathogenesis or in regulating antiviral responses.

DISCUSSION

In rhesus macaques, SFTSV infection caused mild increases in body temperature, mimicking fever seen in patients with SFTS [6, 7], but did not cause death or obvious gastrointestinal, hemorrhagic, or central nervous system symptoms, which are seen in severe cases of SFTS in humans. Comprehensive comparison of the magnitude and dynamics of viremia, hematological and

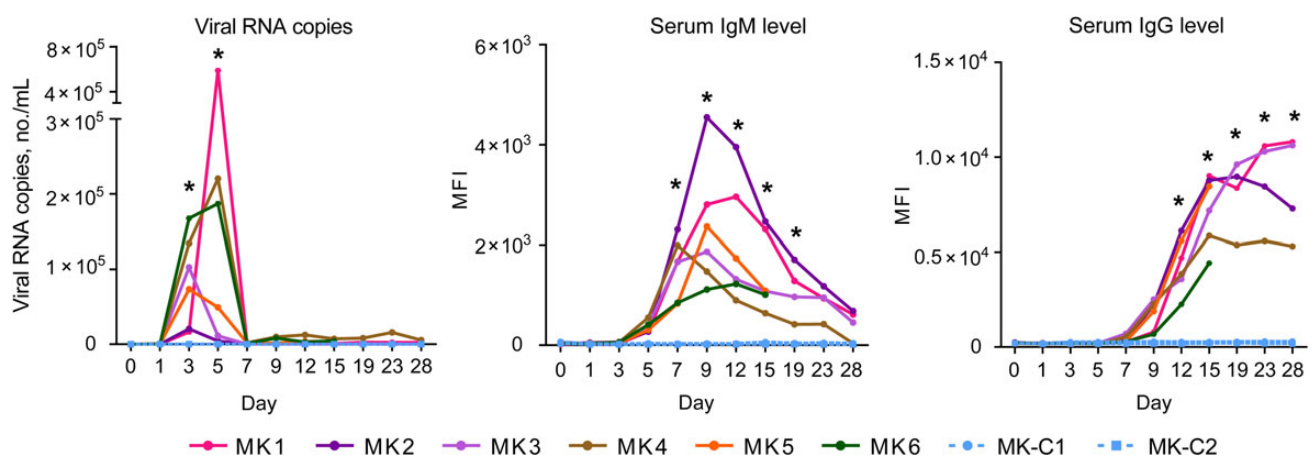


Figure 2. Kinetics of viral RNA copies and virus-specific immunoglobulin M (IgM) and immunoglobulin G (IgG) antibody responses in SFTS virus-infected macaques. Numbers of viral RNA copies in blood were detected by quantitative real-time polymerase chain reaction assays. Levels of virus-specific IgM and IgG antibodies in plasma were tested by Luminex assays. * $P < .05$ between the infected group (MK1–6) and the control group (MK-C1 and MK-C2) at a given time point. Abbreviation: MFI, mean fluorescence intensity.

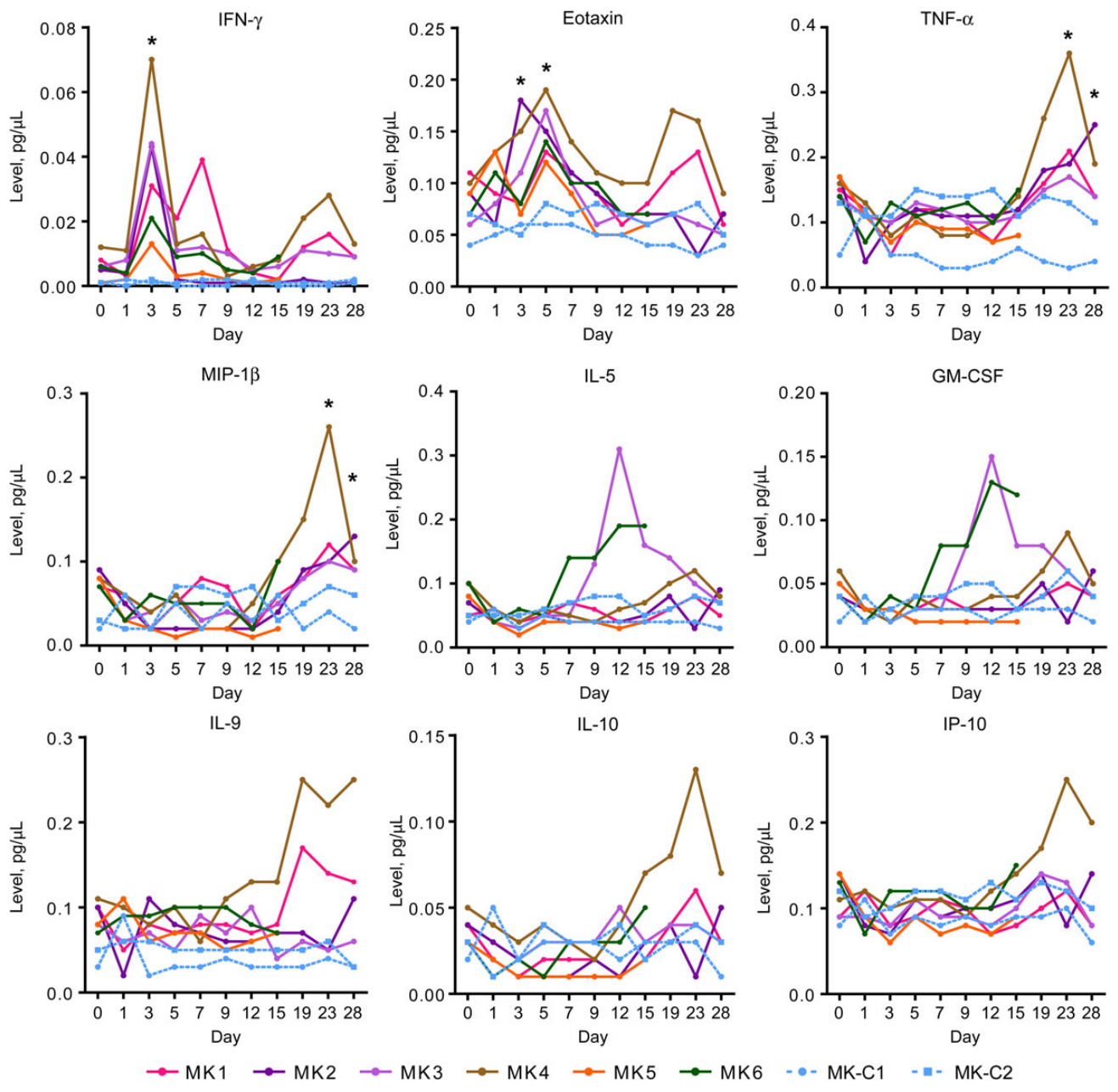


Figure 3. Kinetics of proinflammatory cytokines in SFTS virus-infected rhesus macaques. Plasma levels of cytokines were quantified by multiplex Luminex assays. **P* < .05 between the infected group (MK1–6) and the control group (MK-C1 and MK-C2) at a given time point. Abbreviations: GM-CSF, granulocyte macrophage colony-stimulating factor; IFN- γ , interferon γ ; IL-5, interleukin 5; IL-9, interleukin 9; IL-10, interleukin 10; IP-10, interferon γ -inducible protein; MIP-1 β , macrophage inflammatory protein 1 β ; TNF- α , tumor necrosis factor α .

biochemical parameters, and antibody and cytokine responses among macaques, mice, and humans (Table 1) indicates that SFTSV infection in rhesus macaques is similar to that in mice and resembles a mild infection in humans [1, 7, 14, 25].

In SFTSV-infected rhesus macaques, histopathological lesions were identified in the liver and kidney during the late phase of infection and had similar pathological features as those observed in infected mice [14]. In an autopsy report for

a patient who died from SFTS during the acute phase of infection, mild microvesicular fatty changes and mild inflammation around portal tracts were found in the liver, and subepithelial hemorrhage was observed in the kidneys [13]. Intriguingly, major histopathological lesions were identified in the lymph nodes in the fatal SFTS case, including depletion of lymphocytes, infiltration of histiocytes, and hemophagocytosis of blood cells [13]. Increased hemophagocytosis was also observed

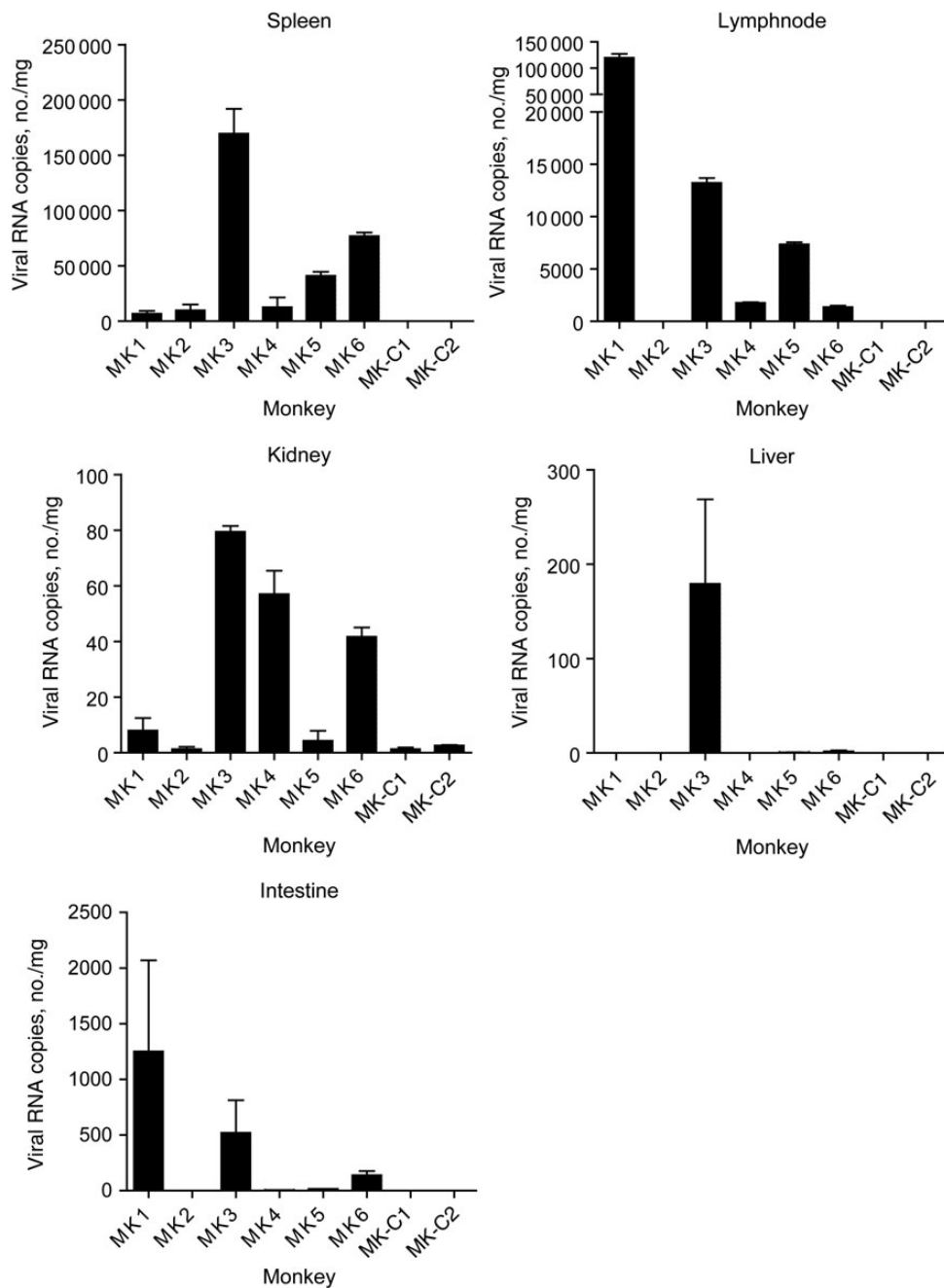


Figure 4. Distribution of the number of viral RNA copies in tissues of SFTS virus–infected macaques. Numbers of viral RNA copies were detected by real-time polymerase chain reaction assays in tissue specimens collected at the experimental end point. In infected macaques (MK1–6), animals MK1–4 were euthanized 4 weeks after inoculation, and animals MK5 and MK6 were euthanized 2 weeks after inoculation. Macaques in the control group (MK-C1 and MK-C2) were euthanized at 4 weeks.

in the spleen in the fatal SFTS case. Increased infiltration of tissue by mononuclear phagocytes and abnormally enhanced phagocytic capacity of phagocytes in the secondary lymphoid organs were similarly observed in mice, with increased infiltration of F4/80-positive macrophages and enhanced phagocytosis of platelets in the spleen during the early phase of infection [14]. It is not known whether the lymph nodes of infected mice

presented similar pathological characteristics because lymph nodes were not examined in the previous mouse studies. Although no obvious pathology was observed in lymph nodes of macaques collected in the late phase of infection, decreased counts of red blood cells and platelets in peripheral blood in the early phase of infection may reflect an enhanced consumption by tissue phagocytes in secondary lymphoid organs.

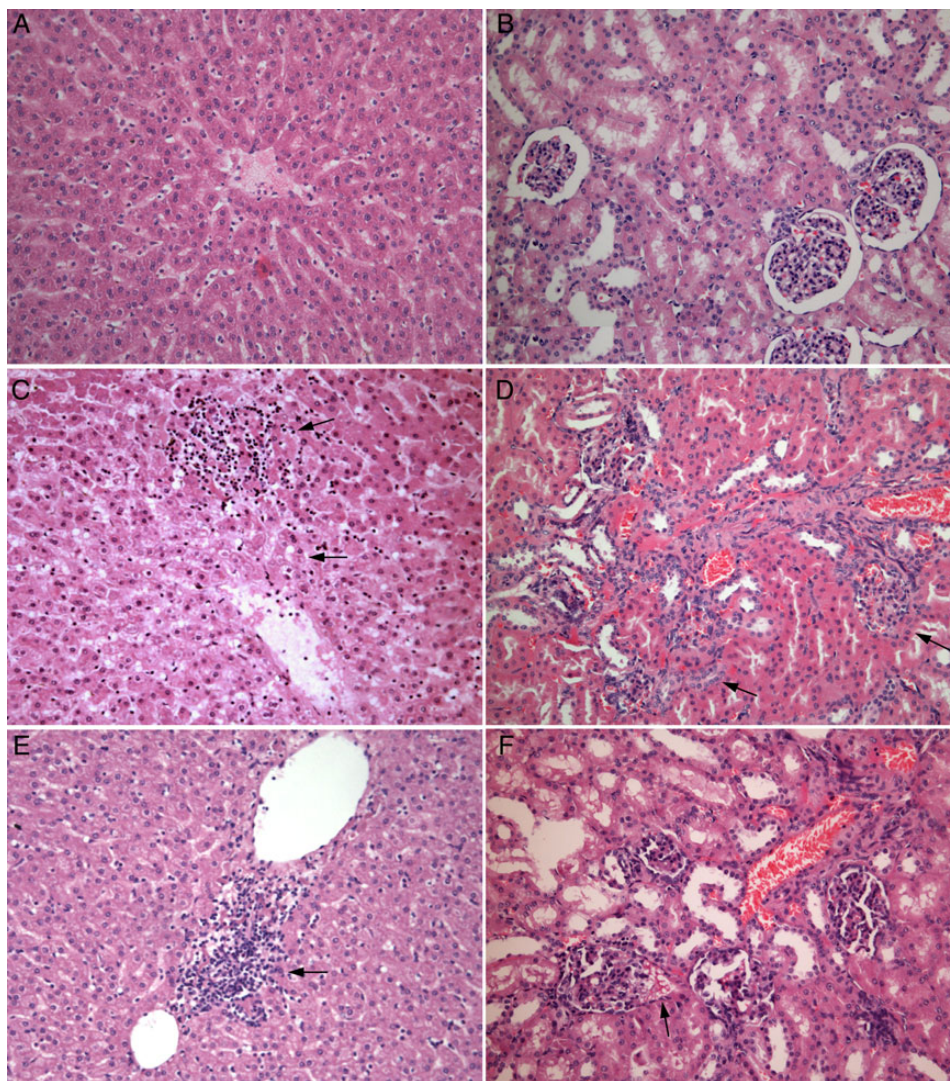


Figure 5. Histopathological lesions in the livers and kidneys of SFTSV (SFTSV)-infected macaques. Representative hematoxylin-eosin–stained tissue sections in control macaques (*A* and *B*) and SFTSV-infected macaques (*C–F*) are shown. In the livers of SFTSV-infected macaques, typical histopathological lesions are intralobular hepatocyte necrosis (arrow at top; *C*), hepatocyte degeneration (arrow at bottom; *C*), and bridging necrosis with infiltration of inflammatory cells in the portal area (arrow; *E*). In the kidneys of SFTSV-infected macaques, typical histopathological lesions are glomerular hypercellularity (arrow at right; *D*), mesangial thickening (arrow at left; *D*), and congestion in the Bowman space (arrow; *F*).

Therefore, these findings suggest that hemophagocytosis occurring in the early phase of infection may be a major cause of SFTSV pathogenesis. Hemophagocytosis can be caused by viral infections, such as Epstein-Barr virus, cytomegalovirus, human immunodeficiency virus, and influenza virus A(H1N1) [26, 27], and is accompanied by a variety of clinical presentations, including fever, acute liver failure, anemia, and thrombocytopenia, as well as cutaneous and neurological symptoms [26]. Excessively proliferated and activated macrophages infiltrate the lymph nodes and spleen and abnormally hemophagocytose various blood cells in these organs [26, 27]. Activated macrophages can also produce large amounts of inflammatory cytokines to cause secondary organ damage [26].

Given previous findings that SFTSV can adhere to platelets [14], it is plausible that, in SFTSV infection, the virus might initially adhere to blood cells, such as red blood cells and/or platelets, inducing their phagocytosis by tissue phagocytes located in secondary lymphoid organs and leading to a decrease in peripherally circulating blood cells. Virus engulfed in tissue phagocytes may then use host cells to rapidly proliferate and cause viremia. This invasion process may also stimulate the production of IFN- γ and other inflammatory cytokines to activate host immune responses and clear the virus, while secondary damage of organs may occur during this process. In immunocompetent animals, virus was efficiently cleared in the early phase of infection, and transient histopathological lesions

were resolved in the late phase, similar to patients with SFTS with mild infection who had viremia and various symptoms in the acute phase and thereafter recovered without sequelae. However, in fatal SFTS cases, most commonly in elderly individuals [6, 7], the immune system may not be sufficiently efficient to clear the virus in the acute phase. Thus, the virus could continue to proliferate at high titers and cause persistent activation of tissue phagocytes, dramatically enhancing hemophagocytosis and cytokine storms, which could then lead to severe dysfunction of multiple organs and, eventually, to death.

The difference in infection features observed between macaques and humans may be due to many factors, including inherent differences in genetic background, analysis at different stages of infection, and different virus strains, infection routes, and exposure doses. Individual variation among infected macaques may be due to the differing genetic backgrounds in outbred nonhuman primates. In fact, SFTSV infection in individual patients also varied from asymptomatic infection to mild infection, severe disease, and death [6, 28, 29], suggesting that host factors may play critical roles in determining disease severity. Individual variation in experimental SFTSV infection in macaques may also depend on virus strains, inoculation route, exposure dose, and macaque species, as well as on the passage generation of virus. For example, the first study describing an infection of nonhuman primates with Rift Valley fever virus (RVFV) reported febrile responses and leukocytopenia but not death [30]. Later studies found that Egyptian viral strains of RVFV were more pathogenic for macaques [31]. The marmoset (*Callithrix jacchus*), a New World primate species, was more susceptible to RVFV infection and had more-marked changes in clinical chemistry and hematological findings than rhesus macaques [19]. RVFV-infected nonhuman primates do not produce a uniformly fatal infection, and <20% of rhesus macaques infected with RVFV develop severe disease [31, 32].

In our study, to minimize individual variation, 8 macaques have the same sex and comparable age and weight. To mimic the infection of humans by tick bite, intramuscular injection was used to inoculate SFTSV, which has been shown in mice to be as efficient as subcutaneous injection in inducing infection of tick-borne viruses, including SFTSV and Crimean-Congo hemorrhagic fever virus [14, 33]. Furthermore, given that macaques have diverse genetic backgrounds and thus may have different infection features, we inoculated 6 macaques with SFTSV to capture the range of possible disease features. Before this study, there was no information on the progression of SFTSV infection in macaques. Because most patients with SFTS recovered in 2–4 weeks [6], 4 macaques were comprehensively analyzed at various time points throughout 4 weeks and followed by an end-point necropsy. Patients with severe SFTS commonly died within 2 weeks after disease onset [6], so we designated 2 macaques for

early phase necropsy if severe symptoms appeared within 2 weeks. Because no severe symptoms appeared, these 2 macaques were euthanized at 2 weeks, in the middle of the infection course. This study design allowed us to perform a complete dynamic analysis on virus clearance, hematological and biochemical parameters, and immune responses from the earliest point of SFTSV infection in macaques. However, because of a lack of obvious disease symptoms, we were not able to perform necropsy during the most severe stage of disease, when significant histopathological lesions might be identified. Additionally, we could not identify an association between viremia and any parameters or cytokines, as has been revealed in population studies. This may be due to our limited sample size of 6 infected macaques [6, 7] or to individual variations in viremia, laboratory parameters, and cytokine responses.

In conclusion, this study comprehensively describes the infection of a novel phlebovirus, SFTSV, in nonhuman primates. We show that SFTSV can infect rhesus macaques and induce infection features and immune responses that mirror mild infection in humans. Although this study has several limitations in population size, infection route, and a lack of examination of histological lesions during the early phase of infection, it supplies useful information for better understanding SFTSV pathogenesis. Further studies in macaques are needed, including testing different macaque species, infectious routes, inoculation doses, and virus strains, as well as necropsies during earlier time points of infection. For practical reasons, *in vivo* studies to investigate disease pathogenesis and variability of clinical presentations are limited in humans. Thus, this study of nonhuman primates advances our understanding of the pathogenesis of SFTSV infection and will eventually facilitate development of novel treatment strategies and vaccines to combat this emerging bunyavirus.

Supplementary Data

Supplementary materials are available at *The Journal of Infectious Diseases* online (<http://jid.oxfordjournals.org>). Supplementary materials consist of data provided by the author that are published to benefit the reader. The posted materials are not copyedited. The contents of all supplementary data are the sole responsibility of the authors. Questions or messages regarding errors should be addressed to the author.

Notes

Acknowledgments. We thank Brad Jones, Ryan Park, and Sophia Rois Geffen, for help in the manuscript writing and editing process.

Financial support. This work was supported by the National Natural Science Foundation of China (grants 81261120420 and 81101301) and the National Key Program on Basic Research Project (973 Program), via the Ministry of Science and Technology (grant 2011CB504700).

Potential conflicts of interest. All authors: No reported conflicts.

All authors have submitted the ICMJE Form for Disclosure of Potential Conflicts of Interest. Conflicts that the editors consider relevant to the content of the manuscript have been disclosed.

References

1. Yu XJ, Liang MF, Zhang SY, et al. Correspondence and requests for materials should be addressed to Fever with thrombocytopenia associated with a novel bunyavirus in China. *N Engl J Med* **2011**; 364:1523–32.
2. Feldmann H. Truly emerging—a new disease caused by a novel virus. *N Engl J Med* **2011**; 364:1561–3.
3. Niu G, Li J, Liang M, et al. Severe fever with thrombocytopenia syndrome virus among domesticated animals, China. *Emerg Infect Dis* **2013**; 19:756–63.
4. Gai Z, Liang M, Zhang Y, et al. Person-to-person transmission of severe fever with thrombocytopenia syndrome bunyavirus through blood contact. *Clin Infect Dis* **2012**; 54:249–52.
5. Bao CJ, Guo XL, Qi X, et al. A family cluster of infections by a newly recognized bunyavirus in eastern China, 2007: further evidence of person-to-person transmission. *Clin Infect Dis* **2011**; 53:1208–14.
6. Gai ZT, Zhang Y, Liang MF, et al. Clinical progress and risk factors for death in severe fever with thrombocytopenia syndrome patients. *J Infect Dis* **2012**; 206:1095–102.
7. Sun Y, Jin C, Zhan F, et al. Host cytokine storm is associated with disease severity of severe fever with thrombocytopenia syndrome. *J Infect Dis* **2012**; 206:1085–94.
8. Ding F, Zhang W, Wang L, et al. Epidemiologic features of severe fever with thrombocytopenia syndrome in China, 2011–2012. *Clin Infect Dis* **2013**; 56:1682–3.
9. Qu J, Zhang S, Li JD, Li DX. Epidemic situation and surveillance on SFTS in China, 2011–2012. *Zhonghua Shi Yan He Lin Chuang Bing Du Xue Za Zhi* **2013**; 27:257–9.
10. Kim KH, Yi J, Kim G, et al. Severe fever with thrombocytopenia syndrome, South Korea, 2012. *Emerg Infect Dis* **2013**; 19:1892–4.
11. McMullan LK, Folk SM, Kelly AJ, et al. A new phlebovirus associated with severe febrile illness in Missouri. *N Engl J Med* **2012**; 367:834–41.
12. Mourya DT, Yadav PD, Basu A, et al. Malsoor virus, a novel bat phlebovirus, is closely related to severe fever with thrombocytopenia syndrome virus and heartland virus. *J Virol* **2014**; 88:3605–9.
13. Takahashi T, Maeda K, Suzuki T, et al. The first identification and retrospective study of severe Fever with thrombocytopenia syndrome in Japan. *J Infect Dis* **2014**; 209:816–27.
14. Jin C, Liang M, Ning J, et al. Pathogenesis of emerging severe fever with thrombocytopenia syndrome virus in C57/BL6 mouse model. *Proc Natl Acad Sci U S A* **2012**; 109:10053–8.
15. Klingstrom J, Falk KI, Lundkvist A. Delayed viremia and antibody responses in Puumala hantavirus challenged passively immunized cynomolgus macaques. *Arch Virol* **2005**; 150:79–92.
16. Hooper JW, Custer DM, Thompson E, Schmaljohn CS. DNA vaccination with the Hantaan virus M gene protects hamsters against three of four HFRS hantaviruses and elicits a high-titer neutralizing antibody response in rhesus monkeys. *J Virol* **2001**; 75:8469–77.
17. Klingstrom J, Stoltz M, Hardestam J, Ahlm C, Lundkvist A. Passive immunization protects cynomolgus macaques against Puumala hantavirus challenge. *Antivir Ther* **2008**; 13:125–33.
18. Klingstrom J, Plyusnin A, Vaheri A, Lundkvist A. Wild-type Puumala hantavirus infection induces cytokines, C-reactive protein, creatinine, and nitric oxide in cynomolgus macaques. *J Virol* **2002**; 76:444–9.
19. Smith DR, Bird BH, Lewis B, et al. Development of a novel nonhuman primate model for Rift Valley fever. *J Virol* **2012**; 86:2109–20.
20. McElroy AK, Bray M, Reed DS, Schmaljohn CS. Andes virus infection of cynomolgus macaques. *J Infect Dis* **2002**; 186:1706–12.
21. Yanagihara R, Amyx HL, Lee PW, Asher DM, Gibbs CJ Jr, Gajdusek DC. Experimental hantavirus infection in nonhuman primates. *Arch Virol* **1988**; 101:125–30.
22. Sun Y, Liang M, Qu J, et al. Early diagnosis of novel SFTS bunyavirus infection by quantitative real-time RT-PCR assay. *J Clin Virol* **2012**; 53:48–53.
23. Knodell RG, Ishak KG, Black WC, et al. Formulation and application of a numerical scoring system for assessing histological activity in asymptomatic chronic active hepatitis. *Hepatology* **1981**; 1:431–5.
24. Canales BK, Reyes L, Reinhard MK, Khan SR, Goncalves CG, Meguid MM. Renal glomerular and tubular injury after gastric bypass in obese rats. *Nutrition* **2012**; 28:76–80.
25. Deng B, Zhou B, Zhang S, et al. Clinical features and factors associated with severity and fatality among patients with severe fever with thrombocytopenia syndrome Bunyavirus infection in Northeast China. *PLoS One* **2013**; 8:e80802.
26. Usmani GN, Woda BA, Newburger PE. Advances in understanding the pathogenesis of HLH. *Br J Haematol* **2013**; 161:609–22.
27. Maakaroun NR, Moanna A, Jacob JT, Albrecht H. Viral infections associated with haemophagocytic syndrome. *Rev Med Virol* **2010**; 20:93–105.
28. Wang Y, Deng B, Zhang J, Cui W, Yao W, Liu P. Person-to-person asymptomatic infection of severe fever with thrombocytopenia syndrome virus through blood contact. *Intern Med* **2014**; 53:903–6.
29. Li Z, Hu J, Bao C, et al. Seroprevalence of antibodies against SFTS virus infection in farmers and animals, Jiangsu, China. *J Clin Virol* **2014**; 60:185–9.
30. Easterday BC. Rift valley fever. *Adv Vet Sci* **1965**; 10:65–127.
31. Peters CJ, Jones D, Trotter R, et al. Experimental Rift Valley fever in rhesus macaques. *Arch Virol* **1988**; 99:31–44.
32. Morrill JC, Jennings GB, Johnson AJ, Cosgriff TM, Gibbs PH, Peters CJ. Pathogenesis of Rift Valley fever in rhesus monkeys: role of interferon response. *Arch Virol* **1990**; 110:195–212.
33. Zivcec M, Srafinetz D, Scott D, Robertson S, Ebihara H, Feldmann H. Lethal Crimean-Congo hemorrhagic fever virus infection in interferon alpha/beta receptor knockout mice is associated with high viral loads, proinflammatory responses, and coagulopathy. *J Infect Dis* **2013**; 207:1909–21.
34. Andrade MC, Ribeiro CT, Silva VF, et al. Biologic data of *Macaca mulatta*, *Macaca fascicularis*, and *Saimiri sciureus* used for research at the Fiocruz primate center. *Mem Inst Oswaldo Cruz* **2004**; 99:581–9.
35. Hom GJ, Bach TJ, Carroll D, et al. Comparison of cardiovascular parameters and/or serum chemistry and hematology profiles in conscious and anesthetized rhesus monkeys (*Macaca mulatta*). *Contemp Top Lab Anim Sci* **1999**; 38:60–4.
36. Rosenblum IY, Coulston F. Normal range and longitudinal blood chemistry and hematology values in juvenile and adult rhesus monkeys (*Macaca mulatta*). *Ecotoxicol Environ Saf* **1981**; 5:401–11.